Chapter 13
Modern Approach of Hydroxyapatite Based Composite for Biomedical Applications

Che Azurahanim Che Abdullah, Eszarul Fahmi Esa, and Farinawati Yazid

13.1 Introduction

This chapter presents an overview related to the modern approach of hydroxyapatite (HA) based composite for biomedical applications. Composite refers to a heterogeneous combination made up of two or more materials having different composition, properties and morphology in order to produce new materials with specific physical, chemical and mechanical characteristics (Salernitano and Migliaresi 2003). Simply speaking, the composite contains at least two or more components known as matrix and reinforcement. Biocomposites, on the other hand, refers to the blends of different materials based on their biocompatibility for various applications. Different types of composites, already in use or currently investigated for various biomedical applications, are presented in this chapter. The focus will be on the types of HA based composite, synthesis and fabrication approaches, characterization, various biomedical applications, the cell-material interactions and its bioactivity and biocompatibility.

C. A. C. Abdullah (✉)
Department of Physics, Faculty of Science, Universiti Putra Malaysia, Serdang, Selangor, Malaysia

Material Synthesis and Characterization Laboratory, Institute of Advanced Technology, Universiti Putra Malaysia, Serdang, Selangor, Malaysia

Laboratory of Cancer Research UPM - MAKNA (CANRES), Institute of Bioscience, Universiti Putra Malaysia, Serdang, Selangor, Malaysia
e-mail: azurahanim@upm.edu.my

E. F. Esa
Department of Physics, Faculty of Science, Universiti Putra Malaysia, Serdang, Selangor, Malaysia

F. Yazid
Center of Family Oral Health, Faculty of Dentistry, Universiti Kebangsaan, Jalan Raja Muda Abdul Aziz, Kuala Lumpur, Malaysia

S. Siddiquee et al. (eds.), *Composite Materials: Applications in Engineering, Biomedicine and Food Science*, https://doi.org/10.1007/978-3-030-45489-0_13

HA based composite also known as bioceramics composite and been used for the past several years for various biomedical applications and recently its being used mainly in tissue engineering. Calcium phosphate or single-phase HA based composite have been widely used for the past thirty years. The advantages offer by the HA based composites consist of high compressive strength, comparative inertness towards body fluids, its attractive appearance, biodegradability, and high biocompatibility led to the use of bioceramics composite in dental and orthopaedic related biomedical applications. The structure of this chapter is organized as follows. In Sect. 13.2, classifications of the HA based composite materials are described. This is followed by a description of the modern synthesis or fabrication and characterization approaches (Sects. 13.3 and 13.4). Section 13.5 deals with current applications of HA based composite in biomedical focusing on the ideal properties and cell-material interaction. Concluding remarks are offered in the last Sect. 13.6.

13.2 Classification of Hydroxyapatite (HA) Based Composites

HA based composite used mainly in biomedical applications can be classified into various classifications. Herein, the main four classification consist of metal/metal oxide matrix HA based composite, polymer matrix HA based composite, carbonaceous HA based composite, and the hybrid HA based composite (Fig. 13.1). In terms of polymer matrix, HA based composite can be further divided into natural and synthetic polymer.

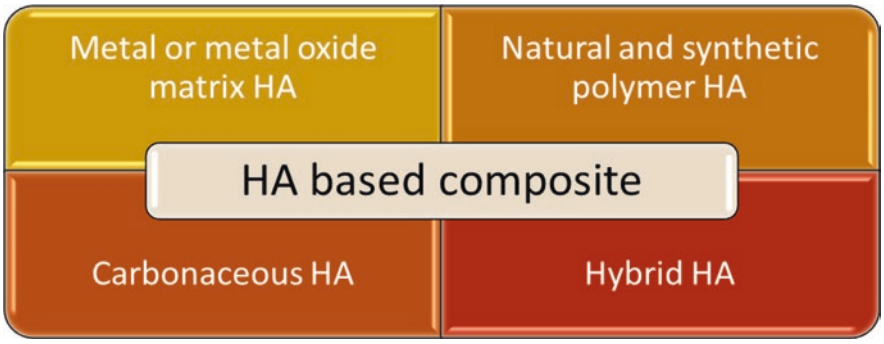

Fig. 13.1 Classification of hydroxyapatite (HA) composites

13.2.1 Metal Matrix Hydroxyapatite (HA) Based Composite

HA having component comparable to crystal structure of bone offers both bioactivity and compatibility. The major bottleneck related to the application of HA mainly due to their low fracture toughness and flexural strength. In order to enhance the mechanical properties of HA, metal and metal oxide such as magnesium, titanium dioxide, zirconia, alumina, and iron oxide usually incorporated in order to reinforce the prepared HA-based composites. The metal matrix HA based composite possess good tensile strength, high Young's modulus, high strength and highly resistance to corrosion. For biomedical application, the HA composite should be biodegradable and non-toxic (Bommala et al. 2018). Table 13.1 listed several types of metal and metal oxide previously used in preparing HA based composite for various biomedical application.

13.2.2 Polymer Matrix Hydroxyapatite (HA) Based Composite

Reinforcement can be achieved by incorporating HA with either natural or synthetic polymer the prepared HA-based composites (Fig. 13.2). Polymers provide various properties as a matrix for bone tissue engineering applications. Natural polymer-based composites received more attention than synthetic polymer composites owing to the biocompatible and biodegradable properties offered by natural polymers. Other advantages included biological recognition, good attachment to cells and having the ability to be degraded and resorbed by the body (Venugopal et al. 2010). Chitosan, chitin, collagen, gelatin and polylactic acid (PLA), hylauronic acid derivatives, starch, fibrin gels, silk and lignocelluloses are among popular natural polymer in preparing composites for medical application.

Table 13.1 Metal and metal oxide used in preparing HA based composite

Types of Metal or Metal Oxide	Applications	References
Titanium (Ti) / Titanium Dioxide (TiO_2)	Implant	Oleiwi et al. (2015); Lim et al. (2001)
Magnesium (Mg) / Magnesium Oxide (MgO)	Bone replacement	Khanra et al. (2010)
Zinc (Zn) / Zinc Oxide (ZnO)	Bone implant, Antibacterial Biomaterial	Begam et al. (2017); Suparto and Kurniawan (2019)
Lanthanum (La)	Bone replacement	Yang et al. (2007)
Zirconia (Zr) / Zirconia dioxide (ZrO_2)	Bone scaffold, Orthopaedic and Dental Prosthesis	An et al. (2012), Zhang et al. (2006), Matsumoto et al. (2011), Sung et al. (2007)
Iron Oxide (IO)	Bone cancer therapy	Sneha and Sundaram (2015)
Alumina (Al_2O_3)	Bone scaffold	Raj et al. (2018)

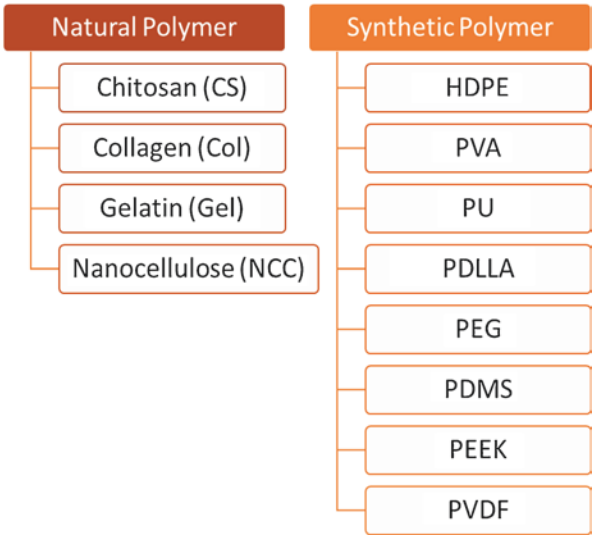

Fig. 13.2 Several examples of natural and synthetic polymer incorporated to produce HA-based polymer composites

Apart from biocompatible and biodegradable, antimicrobial and antioxidant properties of the prepared HA based composites widely expand their application in various fields ranging from food nutrition, biomedical engineering up to pharmaceutical. The composites also should mimic the behavior of the replaced tissue, providing an ideal when in contact with the tissue and capable to be degraded progressive as soon as the regeneration process ended. However, these naturally derived polymers have several drawbacks such as instability and immunogenicity from batch to batch. So, synthetic polymers with modifiable properties such as polyvinyl alcohol (PVA), polyurethane (PU), poly-d, l-lactic acid (PDLLA), polyethylene glycol (PEG), polydimethylsiloxane (PDMS), polyether ether ketone (PEEK) and thermoplastic polyvinylidene difluoride (PVDF) are among synthetic polymers usually used to create HA based composite as they offer exceptional applicability. The advantages offered by synthetic polymer consist of controlled mechanical properties, biodegradable, and reproducible for an extensive production.

13.2.3 Carbonaceous Hydroxyapatite (HA) Based Composite

Along with the excitement of nanoscience and the diverse applications of carbon-based nanomaterials, researchers worldwide started to utilise different carbonaceous materials to prepare nanocomposites either as a matrix material or as an additional reinforcing material. The carbonaceous materials reported to be bioactive for one or more purposes as it offers high competency for bone tissue engineering

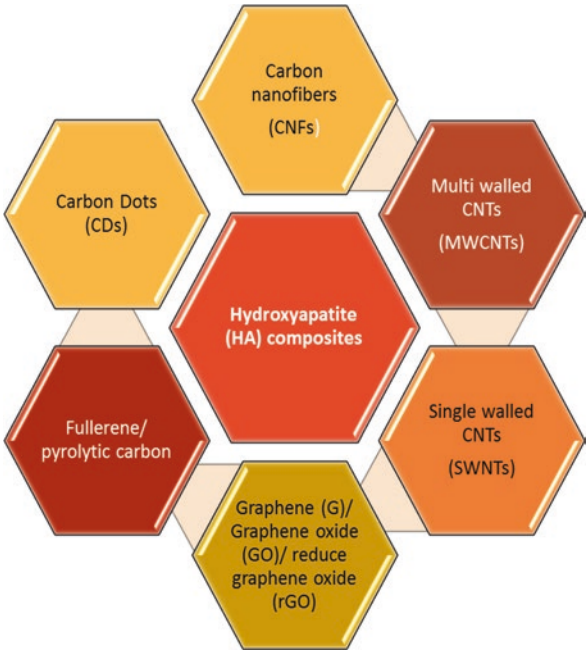

Fig. 13.3 Carbonaceous HA based composites

equipped with biocompatibility with native tissues and antibacterial activity. The incorporation of various carbonaceous materials with HA led to high biocompatibility and excellent structural properties of the prepared nanocomposite. The use of carbonaceous material such as glassy or pyrolytic carbon, fullerenes, carbon nanotubes (CNTs) graphene oxide (GO), carbon dots (CDs) and their derivatives and compositions are unique and innovative trend in creating HA based composites (see Fig. 13.3).

13.2.4 Hybrid Hydroxyapatite (HA) Based Composite

A major challenge in tissue engineering is the development of composite materials capable of promoting the desired cells and tissue behavior (Davis and Leach 2008). So, hybrid HA based composite biomaterials having the capability to synergize the beneficial properties of multiple materials into an outstanding matrix (Bencherif et al. 2013). The hybrid HA prepared by combination of various other materials such as metal or metal oxides with either natural or synthetic polymers or carbonaceous materials. The hybrid composites offer tuneable properties and providing enhancement in cellular and tissue interaction tissue. There are numerous hybrid HA based composite materials (as listed in Fig. 13.4) in order to promote the formation of cell proliferation for tissue engineering applications.

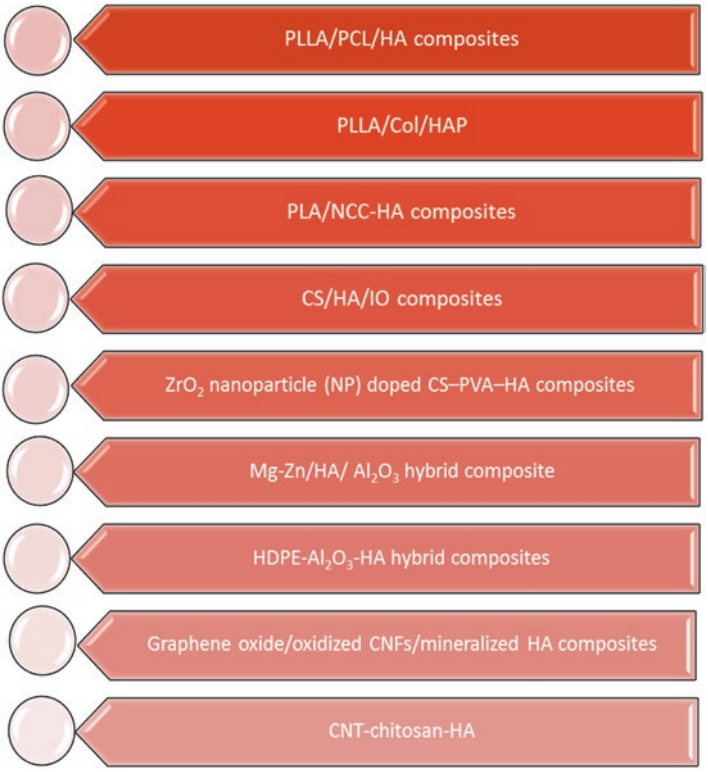

Fig. 13.4 Examples of hybrid HA based composite

13.3 Modern Synthesis and Fabrication Approaches

Owing to the importance of HA based composites in various biomedical applications not limited to tissue regeneration and drug delivery applications. So, various techniques (see Fig. 13.5) have been reported for the preparation of HA based composites (Haider et al. 2017). Two important factors when choosing the synthesis approach are particle size and morphology of the final product of HA. To date, many findings correlated the HA synthesis techniques with the particle size, but very few articles reported the fabrication method and the morphology control of HA based composites.

The commonly used techniques for the preparation of HA based composite including biometrics, freeze thawing, electronspinning, electrospraying, chemical precipitation, hydrothermal, solid state synthesis at high temperatures, microwave irradiation, surfactant-assisted precipitation, wet chemical synthesis, powder metallurgy, ultrasound cavitation, solvent casting, sol-gel method and green synthesis

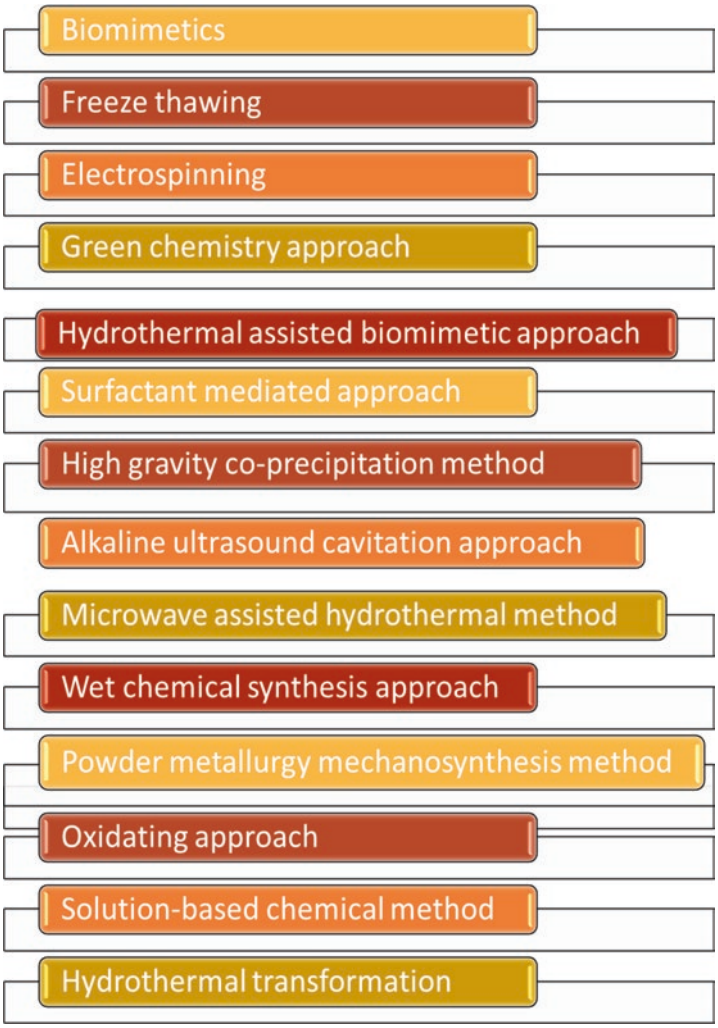

Fig. 13.5 Modern synthesis approaches in the fabrication of hydroxyapatite (HA) based composites

approach. Chemical precipitation, hydrothermal and sol–gel technique listed as the most frequently approach in the HA based nanocomposite fabrications. Table 13.2 summarized several common methods and the developed HA based composites. Until now researchers still are investigating for the method to prepare composites of HA with the right stoichiometry and having both high crystallinity and aspect ratio. So far, only conventional wet mechano-chemical methods have been reported to have the ability to control the stoichiometry of the final product.

Table 13.2 Several common methods and example of the developed hydroxyapatite (HA) based composites

Fabrication techniques of HA composites	Composites	References
Biomimetics	Col/HA, CNF/HA, PCL/HA	Lickorish et al. (2004); Wu et al. (2013); Lebourg et al. (2010)
Freeze thaw	PVA/HA, nHA@Fe_2O_3/PVA	Su et al. (2017); Hou et al. (2013)
Electronspinning	PLLA/MWNTs/HA, PLGA/HA, HA-PVP/PEO	Mei et al. (2007); Lao et al. (2011); Zhou et al. (2014)
Chemical precipitation	Nano-Al_2O_3 /HA	Zhang et al. (2016)
Hydrothermal	HA/Alumina and HA/MgO, SHA/rGO, GO/HA	Vijayalakshmi and Dhanasekaran (2017); Edwin et al. (2019); Rodríguez-González et al. (2018)
Microwave irradiation	PVOH/CNT/HA, Ag@Zn/HA, CS-HA	Lim (2018); Nedunchezhian et al. (2016); Sukhodub et al. (2018)
Sol-gel method	ZrO_2/Hap, TEOS/PDMS/HA, AMWCNT/HA	Bollino et al. (2017); Luo et al. (2015); Ji et al. (2015)
Solvent casting	P3HB/HA, p-PLLA/HA	Saadat et al. (2015); Dou et al. (2018)

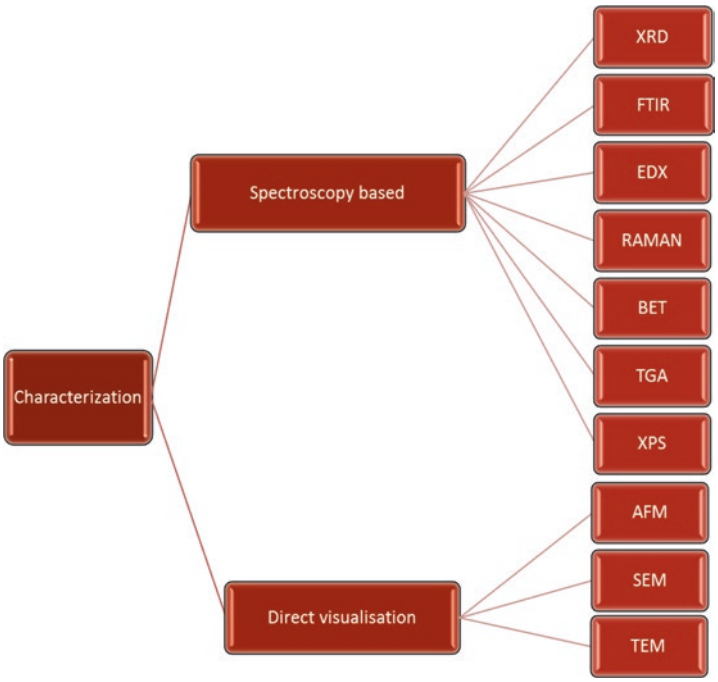

Fig. 13.6 Various characterization methods to evaluate the hydroxyapatite (HA) based composites

Table 13.3 Characterization methods and main findings of various HA based composites

X-Ray Diffraction Analysis (XRD) -degree of crystallinity -crystallite size	**Metal or metal oxide HA** - Diffraction peak of HA appeared in the composite at 2θ = 31.5°, 50° and 60° after samples dried at 100 °C (Bouiahya et al. 2019). - Crystallinity of the composite decreases and the crystallite size getting smaller when content of alumina increases (Bouiahya et al. 2019). - The intensity of diffraction peak of HA in Fe-HA became lower due to ion exchange between Fe^{3+} and Ca^{2+} ion. The increment of Fe^{3+} led to the crystallinity decreased (Pai and Yen 2013). - XRD peaks position for La-HA deviated slightly towards lower angle which may be due to distortion in crystal lattice following substitution of La in HA (Mathi et al. 2019)
	Natural or synthetic polymer HA - The addition of HA led to the reduction in terms of crystallinity degree of PCL as shown by the intensity peak of HA compared to PCL (Trakoolwannachai et al. 2019a, b). - Two notable sharp peaks for PEG noticeable at 2θ = 19.1° and 23.2° and peaks for HA is 2θ = 25.9° and 31.7°. As the positions does not overlapped, this indicated that there are no chemical interaction between PEG and HA (Wang et al. 2017). - HA peak in composite appeared at 2θ = 25.9° and growth took place at (002) crystal plane. The PPy diffraction peak disappear due to weak intensity and covered by the background of HA peaks (Huixia et al. 2016)
	Carbonaceous HA - Addition of fMWCNT into the HA found to have effect on the width at half maximum of the peak. As the width increases, it indicates that the crystallinity index decreased meanwhile crystallite size increased (Barabás et al. 2015). - XRD pattern of GO-HA consisted of HA peak at 2θ = 31.8° without any secondary phase. GO diffraction peak wasn't detectable in composite probably due to low concentration of GO or less crystallographic order (Karimi et al. 2019). - The XRD pattern obtained for HA/GO represented by the peaks at 25.87°, 31.42°, 32.11°, 32.52°, 39.62° and 49.42° with crystal plane (002), (211), (112), (300), (202), (310), (222), (213) and (004) was matched with the (JCPDS: No. 09–0432). The formation of well crystallized hexagonal phase of HA grown on two dimensional GO sheet was confirmed (Ramadas et al. 2017)
	Hybrid HA - Typical peak for GO disappear besides crystallinity of HA and PLA decreased in PLA/HA/GO composites due to good dispersion of GO and HA in PLA matrix (Gong et al. 2017). - Diffraction peaks at 38.2°, 44.3°, 64.5°, 77.3° corresponding to planes [1 1 1], [2 0 0], [2 2 0], [3 1 1] of fcc silver particles. The presence of peaks at 20° and 31.7° revealed the characteristic to the presence of crystalline chitosan and n-HA respectively (Saravanan et al. 2011). - Diffraction peak of Cs in composite revealed the semi crystalline nature as the peak was broad at 10°–20° meanwhile n-HA and $nZrO_2$ exhibited crystalline nature which is composite scaffold also corroborated as crystalline phase due to imparted by n-HA and $nZrO_2$ (Balagangadharan et al. 2018).

(continued)

Table 13.3 (continued)

Fourier Transform Infrared Spectroscopy (FTIR) -functional group	**Metal or metal oxide HA** - IR spectra for Al/HA displayed the stretching mode of PO_4 at 1100, 1050, 960 cm^{-1} and bending mode at 605 and 564 cm^{-1} (Bouiahya et al. 2019). - The stretching bond of phosphate observed at wavenumber of 962 cm^{-1} which indicate the formation of HA in composite (Valizadeh et al. 2014). - IR analysis for HA/Fe_3O_4 displays vibration peak of phosphate at wavenumber 569 cm^{-1}, 1044 cm^{-1}, and 1047 cm^{-1} (Vahdat et al. 2019)
	Natural or synthetic polymer HA - FTIR spectra of HA/PCL composites showed strong P-O stretching peak in the wavenumber range 1000–1100 cm^{-1} (Trakoolwannachai et al. 2019a, b). - N-H bending band for chitosan shift slightly due to hydrogen bond with HA and the P-O bending peak at wavenumber of 952 cm^{-1} (Trakoolwannachai et al. 2019a, b). - Specific bending vibration mode of PO_4 at wavenumber of 567 and 603 cm^{-1} while stretching mode vibration at wavenumber of 963, 1035 and 1101 cm^{-1}. Some peaks of HA and PPy in composite slightly shift due to interaction within composite (Huixia et al. 2016)
	Carbonaceous H - The peaks observed at 2920 and 2850 cm^{-1} attributed to ACH symmetric and asymmetric vibrations of GOs. The peak at 1642 cm^{-1} corresponds to the stretching vibration mode of carbonyl group present in the graphene. The bending vibration of phosphate display at wavenumber of 629, 600 and 564 cm^{-1} (Prabhu et al. 2016). - Phosphate absorption band at 610 cm^{-1}, 1037 cm^{-1} and 1091 cm^{-1} indicates the present of HA in composite and peak found at 1730 cm^{-1} related to GO (Karimi et al. 2019). - FTIR spectrum of HA/GO displayed bending vibration band of phosphate at 568 and 601 cm^{-1} meanwhile stretching vibration band were observed at 1099 and 1037 cm^{-1}. The band of C=C and C=O stretching of GO were 1622 and 1722 cm^{-1} respectively (Ramadas et al. 2017)
	Hybrid HA - CsAgHA composite exhibited different modes of phosphate band at 1035, 606, 517 cm^{-1}. Peak at 1610 cm^{-1} corresponds well to NH_2 absorption band in CS. Characteristic peak of C=O is shifted to 1635 cm^{-1} by the coordinative interaction between Ag ions and the NH_2 groups of CS (Yan et al. 2015). - Amine peak of CS displayed at wavenumber of 1656 cm^{-1}. Peak at 1634 cm^{-1}, 1070 cm^{-1} and 572 cm^{-1} correspond to n-HA in composite. Zr-O stretching vibration mode can be observed at wavenumber of 452 cm^{-1} and 416 cm^{-1} (Balagangadharan et al. 2018). - PLA/HA/GO composite displayed characteristic band of C=C vibration at ca. 1617 cm^{-1} indicates that GO successfully introduced in composite. Besides, the appearance of peaks at 1041, 605 and 566 cm^{-1} attributed to phosphate group of HA. Bands at 1184 cm^{-1} and 871 cm^{-1} are due to vibration of C-O-C and C-COO respectively besides bands at 2998 cm^{-1} and 2947 cm^{-1} are assigned to C-H stretching of PLA (Gong et al. 2017)

Table 13.3 (continued)

Scanning Electron microscopy (SEM) -morphology -particle size	**Metal or metal oxide HA** - Surface of La/HA was densely pack and the granules size are very small as well as high agglomeration (Mathi et al. 2019). - HA particle with elongated nanometric (irregular hexagonal) structure was agglomerated and contain silver nanoparticle in its interior (bright spot inside HA). The size of HA in range 100–150 nm long and 40–50 nm wide (Andrade et al. 2016) - Have irregular and porous structure as well as fine and spherical particles for HA/Fe_3O_4 (Vahdat et al. 2019)
	Natural or synthetic polymer HA - Small, irregular-shaped HA distributed homogenously on the surface and within PCL matrix as well as agglomeration occur which enhance its osteoinductive property (Trakoolwannachai et al. 2019a, b). - Scaffold composite showed interconnected pores and pore size within range 200–400 μm. Porosity slightly decreased when HA been incorporated with chitin due to interaction between polymer chains (Kumar et al. 2011). - nHA/CG scaffolds have a porous structure with interconnected pores. Agglomerated nHA particles discernible mostly on the surface of pore wall (Li et al. 2011)
	Carbonaceous HA - GO-nHA particles found to be bigger and having porous structure. However, after fluoride treatment, the particles become smaller and the porosity reduced as fluoride ion started to occupy the composite (Prabhu et al. 2016). - In GNs/HA, HA particles have a rod-like shaped with width around 50 nm and length in range of 100–200 nm (Pang et al. 2014). - C-HA in irregular shaped and rough surface was observed. Irregular surface may enhance the adsorption capacity. The plate-like nanocrystal might be the HA coating on the surface (Long et al. 2019)
	Hybrid HA - CS/n-HA/nAg scaffolds have rough surfaces and porous nature with size ca. 50–100 μm. Size of silver nanoparticles in range of 80–120 nm which distributed in the scaffolds. nHA particles ranging from 80 to 120 nm (Saravanan et al. 2011). - Cs/n-HA/nZrO_2 scaffold have interconnected pores which uniformly spread with size in the range of 55–65 μm. Interconnected porous structure significant in serving as template structure for cell attachment. Bone extracellular matrix formation and provide space for neovascularisation. (Balagangadharan et al. 2018). - PLA/HA/GO scaffold have rough surface with some joints and protuberances on that surface which suggested that GO and HA were attached to the surface of PLA (Gong et al. 2017

(continued)

Table 13.3 (continued)

Energy dispersive X-ray spectroscopy (EDX) -element present -Ca/P molar ratio	**Metal or metal oxide HA** - From EDX analysis concluded that when Al^{3+} ion from aluminium element increase, the Ca/P molar ratio of Al/HA became lower (Bouiahya et al. 2019)
	Natural or synthetic polymer HA - Ca/P molar ratio of nHA/PDLLA composite was 1.62 which is non- stoichiometric, calcium deficient and close to apatite in bone. The apatite mineralisation in surface of NHA/PDLLA is similar to animal bone in main composition (Deng et al. 2008)
	Carbonaceous HA - Ca/P Molar ratio of Go-HA are about 1.7. This result suggested that GO has positive effect on the mineralisation of HA with Ca/P molar ratio close to the pure HA (1.67) (Fathyunes and Khalil-alla 2017)
	Hybrid HA - C, P, O, Ca and Au element are traced in the EDX spectrum for PLA/HA/GO composite which clearly indicate the present of GO and HA in composite. Meanwhile, Au element came from the gold plate used to test sample using SEM measurement. The molar ratio of Ca and P for that composite obtained from EDX measurement is 1.64 which close to natural bone ratio (1.67) (Gong et al. 2017)
Thermogravimetric analysis (TGA) -thermal stability	**Metal or metal oxide HA** - TGA spectra of HA + GA displayed that 6.314% weight loss at 62.69 °C attribute to the presence of water content and 10.76% of weight loss correspond to the phosphate group. Besides, the weight loss of 8.574% at 433.56 °C due to presence of CaOOH. TGA spectra of HA + GA almost similar to HA but different in residual percentage due to presence of Ag metal in residual besides pure CaO. (Bharti et al. 2016). - TGA curve of Al_2O_3-BHA (alumina-bovine hydroxyapatite) display that at evaporation of solvent, adsorbed water and crystal water of boehmite phase (Al-OOH) occurred at ca. 150 °C and 450 °C. Then, transformation of boehmite to α-alumina which the only stable phase of alumina, can be observed at 500–1300 °C. Small amount of BHA converted into β-TCP at 1250–1300 °C (Yelten et al. 2012)
	Natural or synthetic polymer HA - PVAHA composite undergo continuous weight loss until 800 °C due to the degradation of PVA and dehydroxylation of HA. The weight loss due to water occurred up to 200 °C. Between 200 °C and 550 °C, the weight loss caused by degradation of PVA. 50% of PVA in HA has weight loss of 18.01% whereas 1% PVA in composite has weight loss of 7.05%. This finding indicated that the highest weight loss occurred on composite with highest percentage amount of PVA (Hussain et al. 2016). - Incorporation of nHA slightly enhanced the thermal stability of α-chitin. The thermogram of composite showed initial drop at 100 °C due to moisture loss and then it got straightened which indicates that no phase change in composite structure (Kumar et al. 2011)

Table 13.3 (continued)

	Carbonaceous HA - Two major weight loss when heating HA-CNT composite which takes place in air which is attributed to loss of amorphous carbon at 300–400 °C and CNT that typically above 400 °C (Kosma et al. 2013). - TGA curve of fMWCNT-HA composites show that the weight loss of 9.2% at 80–140 °C owing to the elimination of adsorbed water from the surface and pores. At 142–250 °C weight loss of 7.27% due to decomposition of NH_4NO_3 which was the by-product from the synthesis reaction. The composite has good thermal stability according to TGA measurement because of combustion of fMWCNT took place at higher temperature (510–609 °C). The TGA curve of fMWCNT-HA was a multi-stage process as without the formation of stable intermediates (Barabás et al. 2015)
	Hybrid HA - PLA/HA/GO showed the capability of the composite to remain stable without weight loss up to 200 °C. Major weight loss was observed between 240 and 400 °C. Based on the results, when the weight percentage of GO in composite increases, the maximum temperature decomposition become lower. Thermal stability of PLA revealed the enhancement by the addition of GO and HA may be due to interaction between HA, GO and PLA via hydrogen bond and van der Waals force. (Gong et al. 2017)
Brunauer–Emmett–Teller (BET) -pPorosity -specific surface area	**Metal or metal oxide HA** - The composite acted as mesoporous material. BET analysis showed that only moderate increase on specific surface area when high Al introduced to the composite. For lower content of Al, the mesoporosity became more obvious as the enlargement of hysteresis loop seen so obvious. The introduction of aluminium oxide to composite has specific surface area in range of 145 to 206 $m^2\ g^{-1}$, which clearly improve the specific surface area compared to pure HA (ca. $100 m^2 g^{-1}$) (Bouiahya et al. 2019)
	Natural or synthetic polymer HA - BET surface area of PVAHA composite was 41.3–63.7 m^2/g meanwhile for BET nitrogen adsorption/ desorption isotherms of composites showed type IV which a typical type for mesoporous material. (Hussain et al. 2016)
	Carbonaceous HA - BET nitrogen adsorption/desorption for GO-HA displayed type IV which similar to HA and having distinct hysteresis loop when P/P_0 over 0.5, which reveals the characteristic of mesoporous material (Fathyunes and Khalil-alla, 2017)
	Hybrid HA - BET analysis proved that there are mesopores in the GO/HA/CS based composite as from the nitrogen absorption/desorption, the composite has similar structure with that of Type IV isotherm with H3 hysteresis. Based on BJH calculation, that composite consist of large BET surface area and the mesoporous structure distributed at 3.71 nm (Yılmaz et al. 2019)

13.4 Characterization of HA Based Composites

Various characterization techniques have been used to characterize HA based composites. The characterization techniques can be divided into spectroscopic and direct visualization as listed in the Fig. 13.6. Table 13.3 concluded main findings of various HA based composites using both characterization techniques.

13.5 Current Application of Hydroxyapatite (HA) Based Composites

Hydroxyapatite based composites have various biomedical applications especially in tissue engineering. Tissue engineering or regenerative medicine is a field that involves in promoting new tissues or organs to restore defect, lost or damaged tissues and organs by engineered products. The current practice of using bone grafts for treating patients with bone defect resulted from trauma, pathology and congenital disease brings together a few disadvantages. The advancement of tissue engineering has shed a new light for both clinicians and patients involved. The triad of tissue engineering requires stem cells, growth factors and scaffold-based composites. HA based composite is one of the preferred scaffolds due to its similar composition and structure with the natural human bone (Roffi et al. 2017).

13.5.1 Bone Regeneration

Bone disorders due to trauma, congenital deformity and malignancy are one of the pathological areas that require transplantation of bone graft. Bone graft can either be autograft, allograft, xenograft or bone substitutes. However, each graft possesses different drawbacks that hinder optimal outcome after the surgery. Since the last few decades, the advancement in regenerative medicine has gradually being investigated to overcome the limitation of usual practice, including the bone tissue regeneration area. Even though it is difficult to mimic nature, recent scientific and technological findings show promising results to provide an alternative option to the current management. Scaffold, one of the important components in tissue engineering has received tremendous attention among researchers. The search for the right scaffold in bone tissue engineering since past few decades is still ongoing. The ideal scaffold for bone regeneration should have the following properties: biocompatible, bioresorbable, osteoconductive, osteoinductive and structurally similar to the native bone.

13.5.2 Ideal Properties of Scaffolds

Bioceramic such as HA, bioactive glass, zirconia and β-tricalcium phosphate (β-TCP) are mostly used for hard tissue regeneration (Huang et al., 2018; Lukić et al., 2011). HA based scaffolds have been reported to have good biocompatibility and osteoconductivity; suitable for bone regeneration (Hao et al., 2017). Owing to similar chemical composition with native bones HA has become the most common bioceramic used in bone tissue engineering (Mondal et al. 2019; Yang et al. 2019). Scaffolds chosen should mimic the actual microenvironment to allow cells to interact and behave at the optimum condition. Hence, scaffolds properties are essential in determining cellular response and fate (Loh and Choong 2013). There are few requirements for ideal scaffolds required in bone regeneration that include physical properties, biomaterial properties and mechanical properties (Tables 13.4 and 13.5).

Mechanical property of ideal scaffold in bone regeneration requires sufficient mechanical strength in order to maintain the cell integrity until formation of new bone. Newly bone regeneration should withstand loading to prevent shielding as compared to the surrounding native bone (Loh and Choong 2013).

Table 13.4 Physical properties of ideal HA based composite for scaffold in bone regeneration

Properties	Characteristics
Porosity	Pore size Minimum 100 μm in diameter for successful diffusion of nutrients and oxygen (Bose et al. 2012). More than 200 μm for better osteoconduction and up to 500 μm for vascularization (Khojasteh et al. 2016). More than 500 μm might wash away the cells that previously seeded during in vivo application
Interconnectivity	Important to enable proper diffusion of nutrients and metabolic waste into and from deeper part of scaffold for cell viability (Battistella et al. 2012). Important for cell penetration and angiogenesis of cell/scaffold co-culture (Ghassemi et al. 2018)
Porosity	Porous scaffolds will offer high surface area for scaffold-cell interaction; resulted in better cells infiltration and attachment (Loh & Choong 2013). Dense scaffold has excellent mechanical property and less susceptible to breakage, but it has slow dissolution rate

Table 13.5 Biomaterial property of ideal scaffold in bone regeneration

Properties	Characteristics
Biocompatibility	Biocompatible to the cells and environment (Ghassemi et al. 2018)
Osteoconductivity	Bone grows on a scaffold surface
Osteoinductive	Enhance osteogenesis
Bioresorbability	Ability to degrade in vivo, preferably at a controlled rate and eventually providing space for the new bone to grow

13.6 Conclusion and Future Remarks

This chapter reviewed modern approach used in the fabrication of HA based composite for various biomedical applications. Wide range of methods available for fabricating HA based composites have developed in the past few decades. Each of the fabrication methods has its own benefits and drawbacks. Factors need to be taken into consideration include the overall cost, easy and reliable procedures, the performance and characteristic of the end product. The HA composites prepared with either polymers, metals and metal oxide, carbonaceous and the hybrid mixtures have gain worldwide attention due to the outstanding biological properties on top of chemical resemblance to the bone tissues. It is important to consider the ideal properties of the biomaterial in designing the suitable HA based composite for biomedical applications. Future work will focus on the advancement and improvement in fabrication real bone like HA composites with improved mechanical, bioactivity, biocompatibility and osteoconductivity. The cell-material interaction, in vitro and in vivo studies will be the focus in the future.

References

An SH, Matsumoto T, Miyajima H, Nakahira A, Kim KH, Imazato S (2012) Porous zirconia/hydroxyapatite scaffolds for bone reconstruction. Dent Mater 28(12):1221–1231

Andrade FAC, de Oliveira Vercik LC, Monteiro FJ, da Silva Rigo EC (2016) Preparation, characterization and antibacterial properties of silver nanoparticles–hydroxyapatite composites by a simple and eco-friendly method. Ceram Int 42(2):2271–2280

Balagangadharan K, Chandran SV, Arumugam B, Saravanan S, Venkatasubbu GD, Selvamurugan N (2018) Chitosan/nano-hydroxyapatite/nano-zirconium dioxide scaffolds with miR-590-5p for bone regeneration. Int J Biol Macromol 111:953–958

Barabás R, Katona G, Bogya ES, Diudea MV, Szentes A, Zsirka B, Kovács J, Kékedy-Nagy L, Czikó M (2015) Preparation and characterization of carboxyl functionalized multiwall carbon nanotubes–hydroxyapatite composites. Ceram Int 41(10):12717–12727

Battistella E, Mele S, Foltran I, Lesci IG, Roveri N, Sabatino P, Ramondini L (2012) Cuttlefish bone scaffold for tissue engineering: a novel hydrothermal transformation, chemical-physical, and biological characterization. J Appl Biomater Func 10(2):99–106

Begam H, Nandi SK, Chanda A, Kundu B (2017) Effect of bone morphogenetic protein on Zn-HAp and Zn-HAp/collagen composite: a systematic in vivo study. Res Vet Sci 115:1–9

Bencherif SA, Braschler TM, Renaud P (2013) Advances in the design of macroporous polymer scaffolds for potential applications in dentistry. J Periodontal Implant Sci 43(6):251–261

Bharti A, Singh S, Meena VK, Goyal N (2016) Structural characterization of silver-hydroxyapatite nanocomposite: a bone repair biomaterial. Mater Today Proc 3(6):2113–2120

Bollino F, Armenia E, Tranquillo E (2017) Zirconia/hydroxyapatite composites synthesized via sol-gel: influence of hydroxyapatite content and heating on their biological properties. Materials 10(7):757

Bommala VK, Krishna MG, Rao CT (2018) Magnesium matrix composites for biomedical applications: a review. J Magnes Alloy

Bose S, Roy M, Bandyopadhyay A (2012) Recent advances in bone tissue engineering scaffolds. Trends Biotechnol 30(10):546–554

Bouiahya K, Es-saidi I, El Bekkali C, Laghzizil A, Robert D, Nunzi JM, Saoiabi A (2019) Synthesis and properties of alumina-hydroxyapatite composites from natural phosphate for phenol removal from water. Colloid Interfac Sci Commun 31:100188

Davis HE, Leach JK (2008) Hybrid and composite biomaterials in tissue engineering. Topics Multifunct Biomater and Dev 10:1–26

Deng C, Weng J, Lu X, Zhou SB, Wan JX, Qu SX, Feng B, Li XH (2008) Preparation and in vitro bioactivity of poly (D, L-lactide) composite containing hydroxyapatite nanocrystals. Mater Sci Eng C 28(8):1304–1310

Dou T, Jing N, Zhou B, Zhang P (2018) In vitro mineralization kinetics of poly (L-lactic acid)/hydroxyapatite nanocomposite material by attenuated total reflection Fourier transform infrared mapping coupled with principal component analysis. J Mater Sci 53(11):8009–8019

Edwin N, Saranya S, Wilson P (2019) Strontium incorporated hydroxyapatite/hydrothermally reduced graphene oxide nanocomposite as a cytocompatible material. Ceram Int 45(5):5475–5485

Fathyunes L, Khalil-Allafi J (2017) Characterization and corrosion behavior of graphene oxide-hydroxyapatite composite coating applied by ultrasound-assisted pulse electrodeposition. Ceram Int 43(16):13885–13894

Ghassemi T, Shahroodi A, Ebrahimzadeh MH, Mousavian A, Movaffagh J (2018) Current concepts in scaffolding for bone tissue engineering. Archi Bone Joint Surg 6(2):90–99

Gong M, Zhao Q, Dai L, Li Y, Jiang T (2017) Fabrication of polylactic acid/hydroxyapatite/graphene oxide composite and their thermal stability, hydrophobic and mechanical properties. J Asian Ceramic Soc 5(2):160–168

Haider A, Haider S, Han SS, Kang IK (2017) Recent advances in the synthesis, functionalization and biomedical applications of hydroxyapatite: a review. RSC Adv 7(13):7442–7458

Hao Z, Song Z, Huang J, Huang K, Panetta A, Gu Z, Wu J (2017) Scaffold microenvironment for stem cell based bone tissue engineering. Biomater Sci 5(8):1382–1392

Hou R, Zhang G, Du G, Zhan D, Cong Y, Cheng Y, Fu J (2013) Magnetic nanohydroxyapatite/PVA composite hydrogels for promoted osteoblast adhesion and proliferation. Colloids Surf B: Biointerfaces 103:318–325

Huang B, Caetano G, Vyas C, Blaker JJ, Diver C, Bártolo P (2018) Polymer-ceramic composite scaffolds: the effect of hydroxyapatite and β-tri-calcium phosphate. Materials 11(129):2–13

Huixia L, Yong L, Lanlan L, Yanni T, Qing Z, Kun L (2016) Development of ammonia sensors by using conductive polymer/hydroxyapatite composite materials. Mater Sci Eng C 59:438–444

Hussain R, Tabassum S, Gilani MA, Ahmed E, Sharif A, Manzoor F, Shah AT, Asif A, Sharif F, Iqbal F, Siddiqi SA (2016) In situ synthesis of mesoporous polyvinyl alcohol/hydroxyapatite composites for better biomedical coating adhesion. Appl Surf Sci 364:117–123

Ji L, Wang W, Stevens MM, Zhou S, Zhu A, Liang J (2015) A general strategy for the preparation of aligned multiwalled carbon nanotube/inorganic nanocomposites and aligned nanostructures. Mater Res Bull 61:453–458

Karimi N, Kharaziha M, Raeissi K (2019) Electrophoretic deposition of chitosan reinforced graphene oxide-hydroxyapatite on the anodized titanium to improve biological and electrochemical characteristics. Mater Sci Eng C 98:140–152

Khanra AK, Jung HC, Yu SH, Hong KS, Shin KS (2010) Microstructure and mechanical properties of Mg-HAP composites. Bull Mater Sci 33(1):43–47

Khojasteh A, Fahimipour F, Eslaminejad MB, Jafarian M, Jahangir S, Bastami F, Tahriri M, Karkhaneh A, Tayebi L (2016) Development of PLGA-coated β-TCP scaffolds containing VEGF for bone tissue engineering. Mater Sci Eng C 69:780–788

Kosma V, Tsoufis T, Koliou T, Kazantzis A, Beltsios K, De Hosson JTM, Gournis D (2013) Fibrous hydroxyapatite–carbon nanotube composites by chemical vapor deposition: in situ fabrication, structural and morphological characterization. Mater Sci Eng B 178(7):457–464

Kumar PS, Srinivasan S, Lakshmanan VK, Tamura H, Nair SV, Jayakumar R (2011) β-Chitin hydrogel/nano hydroxyapatite composite scaffolds for tissue engineering applications. Carbohydr Polym 85(3):584–591

Lao L, Wang Y, Zhu Y, Zhang Y, Gao C (2011) Poly (lactide-co-glycolide)/hydroxyapatite nanofibrous scaffolds fabricated by electrospinning for bone tissue engineering. J Mater Sci Mater Med 22(8):1873–1884

Lebourg M, Anton JS, Ribelles JG (2010) Hybrid structure in PCL-HAp scaffold resulting from biomimetic apatite growth. J Mater Sci Mater Med 21(1):33–44

Li J, Sun H, Sun D, Yao Y, Yao F, Yao K (2011) Biomimetic multicomponent polysaccharide/nano-hydroxyapatite composites for bone tissue engineering. Carbohydr Polym 85(4):885–894

Lickorish D, Ramshaw JA, Werkmeister JA, Glattauer V, Howlett CR (2004) Collagen–hydroxyapatite composite prepared by biomimetic process. Journal of Biomedical Materials Research Part A: An Official Journal of The Society for Biomaterials, The Japanese Society for Biomaterials, and The Australian Society for Biomaterials and the Korean Society for Biomaterials 68(1):19–27

Lim LS (2018) *Effects of Microwave Radiation on Properties of Polyvinyl Alcohol-Carbon Nanotube-Hydroxyapatite Blends* (Doctoral dissertation, UTAR)

Lim YM, Hwang KS, Park YJ (2001) Sol-gel derived functionally graded TiO2/HAP films on Ti-6Al-4V implants. J Sol-Gel Sci Technol 21(1–2):123–128

Loh QL, Choong C (2013) Three-dimensional scaffolds for tissue engineering: role of porosity and pore size. Tissue Eng Part B Rev 19(6)

Long Y, Jiang J, Hu J, Hu X, Yang Q, Zhou S (2019) Removal of Pb (II) from aqueous solution by hydroxyapatite/carbon composite: preparation and adsorption behavior. In: *Colloids and surfaces A: physicochemical and engineering aspects*

Lukić MJ, Stanković A, Veselinović L, Škapin SD, Bračko I, Marković S, Uskoković D (2011) Chemical precipitation synthesis and characterization of Zr-doped hydroxyapatite nanopowders. In: The thirteenth annual conference YUCOMAT 2011: programme and the book of abstracts. Materials Research Society of Serbia, Belgrade, pp 89–89

Luo Y, Xiao L, Zhang X (2015) Characterization of TEOS/PDMS/HA nanocomposites for application as consolidant/hydrophobic products on sandstones. J Cult Herit 16(4):470–478

Mathi DB, Gopi D, Kavitha L (2019) Implication of lanthanum substituted hydroxyapatite/poly (n-methyl pyrrole) bilayer coating on titanium for orthopedic applications. *Materials today: proceedings*

Matsumoto TJ, An SH, Ishimoto T, Nakano T, Matsumoto T, Imazato S (2011) Zirconia–hydroxyapatite composite material with micro porous structure. Dent Mater 27(11):e205–e212

Mei F, Zhong J, Yang X, Ouyang X, Zhang S, Hu X, Ma Q, Lu J, Ryu S, Deng X (2007) Improved biological characteristics of poly (L-lactic acid) electrospun membrane by incorporation of multiwalled carbon nanotubes/hydroxyapatite nanoparticles. Biomacromolecules 8(12):3729–3735

Mondal S, Hoang G, Manivasagan P, Moorthy MS, Kim HH, Vy Phan TT, Oh J (2019) Comparative characterization of biogenic and chemical synthesized hydroxyapatite biomaterials for potential biomedical application. Mater Chem Phys

Nedunchezhian G, Anburaj DB, Gokulakumar B, Jeyakumar SJ (2016) Microwave assisted synthesis and charecterization of silver and zinc doped hydroxyapatite nanorods from mussel shell (MOLLUSK). Rom J Biophys 26(1)

Oleiwi APDJK, Anaee APDRA, Muhsin LSA (2015) Fabrication, characterization and physical properties of functionally graded Ti/HAP bioimplants. Wulfenia J 22(7):336–348

Pai NS, Yen SK (2013) Preparation and characterization of platinum/iron contained hydroxyapatite/carbon black composites. Int J Hydrog Energy 38(30):13249–13259

Pang P, Liu Y, Zhang Y, Gao Y, Hu Q (2014) Electrochemical determination of luteolin in peanut hulls using graphene and hydroxyapatite nanocomposite modified electrode. Sensors Actuators B Chem 194:397–403

Prabhu SM, Elanchezhiyan SS, Lee G, Khan A, Meenakshi S (2016) Assembly of nano-sized hydroxyapatite onto graphene oxide sheets via in-situ fabrication method and its prospective application for defluoridation studies. Chem Eng J 300:334–342

Raj SV, Rajkumar M, Sundaram NM, Kandaswamy A (2018) Synthesis and characterization of hydroxyapatite/alumina ceramic nanocomposites for biomedical applications. Bull Mater Sci 41(4):93

Ramadas M, Bharath G, Ponpandian N, Ballamurugan AM (2017) Investigation on biophysical properties of hydroxyapatite/Graphene oxide (HAp/GO) based binary nanocomposite for biomedical applications. Mater Chem Phys 199:179–184

Rodríguez-González C, Salas P, López-Marín LM, Millán-Chiu B, De La Rosa E (2018) Hydrothermal synthesis of graphene oxide/multiform hydroxyapatite nanocomposite: its influence on cell cytotoxicity. Mater Res Express 5(12):125023

Roffi A, Krishnakumar GS, Gostynska N, Kon E, Candrian C, Filardo G (2017) The role of three-dimensional scaffolds in treating long bone defects: evidence from preclinical and clinical literature- a systematic review. Biomed Res Int

Saadat A, Karbasi S, Ghader AB, Khodaei M (2015) Characterization of biodegradable P3HB/HA nanocomposite scaffold for bone tissue engineering. Procedia Mater Sci 11:217–223

Salernitano E, Migliaresi C (2003) Composite materials for biomedical applications: a review. J Appl Biomater Biomech 1(1):3–18

Saravanan S, Nethala S, Pattnaik S, Tripathi A, Moorthi A, Selvamurugan N (2011) Preparation, characterization and antimicrobial activity of a bio-composite scaffold containing chitosan/nano-hydroxyapatite/nano-silver for bone tissue engineering. Int J Biol Macromol 49(2):188–193

Sneha M, Sundaram NM (2015) Preparation and characterization of an iron oxide-hydroxyapatite nanocomposite for potential bone cancer therapy. Int J Nanomedicine 10(Suppl 1):99

Su C, Su Y, Li Z, Haq MA, Zhou Y, Wang D (2017) In situ synthesis of bilayered gradient poly (vinyl alcohol)/hydroxyapatite composite hydrogel by directional freezing-thawing and electrophoresis method. Mater Sci Eng C 77:76–83

Sukhodub LB, Kumeda MO, Gapon VI, Sukhodub LF (2018, September) Microwave assisted formation of the chitosan/hydroxyapatite scaffold for bone tissue regeneration. In: *2018 IEEE 8th international conference nanomaterials: application & properties (NAP)*. IEEE, pp 1–4

Sung YM, Shin YK, Ryu JJ (2007) Preparation of hydroxyapatite/zirconia bioceramic nanocomposites for orthopaedic and dental prosthesis applications. Nanotechnology 18(6):065602

Suparto IH, Kurniawan E (2019, August) Synthesis and Characterization of Hydroxyapatite-Zinc Oxide (HAp-ZnO) as Antibacterial Biomaterial. In *IOP conference series: materials science and engineering* (Vol. 599, No. 1, p. 012011). IOP Publishing

Trakoolwannachai V, Kheolamai P, Ummartyotin S (2019a) Characterization of hydroxyapatite from eggshell waste and polycaprolactone (PCL) composite for scaffold material. Compos Part B:106974

Trakoolwannachai V, Kheolamai P, Ummartyotin S (2019b) Development of hydroxyapatite from eggshell waste and a chitosan-based composite: in vitro behavior of human osteoblast-like cell (Saos-2) cultures. Int J Biol Macromol 134:557–564

Vahdat A, Ghasemi B, Yousefpour M (2019) Synthesis of hydroxyapatite and hydroxyapatite/Fe3O4 nanocomposite for removal of heavy metals. Environ Nanotechnol Monit Manage 12:100233

Valizadeh S, Rasoulifard MH, Dorraji MS (2014) Modified Fe3O4-hydroxyapatite nanocomposites as heterogeneous catalysts in three UV, Vis and Fenton like degradation systems. Appl Surf Sci 319:358–366

Venugopal J, Prabhakaran MP, Zhang Y, Low S, Choon AT, Ramakrishna S (2010) Biomimetic hydroxyapatite-containing composite nanofibrous substrates for bone tissue engineering. Philos Trans R Soc A Math Phys Eng Sci 368(1917):2065–2081

Vijayalakshmi V, Dhanasekaran P (2017) Synthesis and structural properties characterization of HA/alumina and HA/MgO Nanocomposite for biomedical applications. Open Access J Trans Med Res 1(4):00020

Wang Y, Liang D, Liu F, Zhang W, Di X, Wang C (2017) A polyethylene glycol/hydroxyapatite composite phase change material for thermal energy storage. Appl Therm Eng 113:1475–1482

Wu M, Wang Q, Liu X, Liu H (2013) Biomimetic synthesis and characterization of carbon nanofiber/hydroxyapatite composite scaffolds. Carbon 51:335–345

Yan Y, Zhang X, Li C, Huang Y, Ding Q, Pang X (2015) Preparation and characterization of chitosan-silver/hydroxyapatite composite coatings onTiO2 nanotube for biomedical applications. Appl Surf Sci 332:62–69

Yang H, Zhang L, Xu KW (2007) The microstructure and specific properties of La/HAP composite powder and its coating. Appl Surf Sci 254(2):425–430

Yang W, Zhou W, Li N, Huang Y, Cheng X, Shua B, Wen B (2019) A clinical study of early intervention with coralline hydroxyapatite on fresh extraction sockets. J Nanosci Nanotechnol 19(11):6956–6960

Yelten A, Yilmaz S, Oktar FN (2012) Sol–gel derived alumina–hydroxyapatite–tricalcium phosphate porous composite powders. Ceram Int 38(4):2659–2665

Yılmaz P, Elif öztürk Er, Bakırdere S (2019) Application of supercritical gel drying method on fabrication of mechanically improved and biologically safe three-component scaffold composed of graphene oxide/chitosan/hydroxyapatite and characterization studies. J Mater Res Technol

Zhang C, Zhang X, Liu C, Sun K, Yuan J (2016) Nano-alumina/hydroxyapatite composite powders prepared by in-situ chemical precipitation. Ceram Int 42(1):279–285

Zhang J, Iwasa M, Kotobuki N, Tanaka T, Hirose M, Ohgushi H, Jiang D (2006) Fabrication of hydroxyapatite–zirconia composites for orthopedic applications. J Am Ceram Soc 89(11):3348–3355

Zhou Y, Qi P, Zhao Z, Liu Q, Li Z (2014) Fabrication and characterization of fibrous HAP/PVP/PEO composites prepared by sol-electrospinning. RSC Adv 4(32):16731–16738